Bull. Mater. Sci., Vol. 37, No. 7, December 2014, pp. 1701–1708. © Indian Academy of Sciences.

Improving electrochemical performance of tin-based anodes formed via oblique angle deposition method

B DENIZ POLAT and OZGUL KELES*
Department of Metallurgical and Materials Engineering, Istanbul Technical University, Maslak, Istanbul 34469, Turkey

MS received 17 December 2013

Abstract. **An oblique angle electron beam co-deposition technique was used to fabricate nanostructured Sn-based thin films: Sn, Cu–Sn and Cu–Sn–C. The morphological and structural properties of the films were observed via scanning electron microscopy (SEM) and thin film X-ray diffraction (XRD) methods. The electrochemical (CV and EIS) and the galvanostatic test results demonstrated that the addition of Cu with or without C affected the electrochemical performance of the thin film positively since Cu and C improved both the mechanical and the electrical properties of the nanostructured Sn thin film electrode. The high cycleability and capacity retention were achieved when the nanostructured Cu–Sn–C thin film was used as an anode material since C increased the mechanical tolerance of the thin film to the volume expansion due to its grain refiner effect. Cu not only improved the electrical conductivity and the adhesion of the film to substrate but also the mechanical tolerance of the film with its ductile property.**

Keywords. **Thin film; oblique angle deposition; lithium ion batteries; anode.**

1. Introduction

In recent times, researchers have been focussing on developing new electrode materials for lithium ion batteries, which have a higher reversible capacity than those of the carbon-based materials. For this purpose, different metals, alloys and intermetallics are studied as negative electrodes (Besenhard *et al* 1997; Wachtler *et al* 2001; Lindsay *et al* 2003; Lee 2007; Kamali and Fray 2011). Among alternatives, tin (Sn) is attractive because it has a higher theoretical retention capacity (994 mAh g^{-1}) than graphite (372 mAh g^{-1}) (Besenhard *et al* 1997; Wachtler *et al* 2001). However, the use of pure Sn as an anode material is restricted because of the high volume change during the cycling test, which in turn causes a loss of the electrical contact among the particles and between the current collector with the thin film, which eventually leads to failure (Kamali and Fray 2011).

To reduce such restrictions, M_xSn_y intermetallic binary systems (where M is an inactive metal, such as Cu, Ni, Fe, Co, Sb, Ag) are used as an anode (Lindsay *et al* 2003; Kawakami and Asao 2005; Mizutani and Inoue 2005; Chen *et al* 2008; Kamali and Fray 2011). Herein, copper (Cu) is preferred mostly due to its high electrical conductivity and its high ductility. These properties are expected to increase the conductivity and the mechanical tolerance of the thin film against the volumetric changes that occur during cycling (Kepler *et al* 1999; Belt *et al* 2003; Kawakami and Asao 2005; Mizutani and Inoue 2005; Zhang *et al* 2011). Cu–Sn phase diagram has various Cu_xSn_y intermetallics:Cu_6Sn_5 is remarkable due to its easy structural decomposition in a conductive Cu matrix (1) and (2) during the lithiation reaction (Kepler *et al* 1999; Jung and Lee 2011). In previous studies, it is shown that the anode made of Cu_6Sn_5 particles has a longer cycle life compared to that of the pure Sn anode because during lithiation, lithium (Li) first reacts to form $Li_2Cu_6Sn_5$ (1), and then with further Li addition $Li_2Cu_6Sn_5$ decomposes into Li–Sn alloys (2) surrounded by Cu matrix (Besenhard *et al* 1986; Kepler *et al* 1999; Thackeray *et al* 2005).

$$10Li + 5\,Cu_6Sn_5 \rightleftharpoons 5Li_2Cu_6Sn_5, \quad (1)$$

$$20Li + Li_2Cu_6Sn_5 \rightleftharpoons 5Li_{4.4}Sn + 6Cu. \quad (2)$$

Nevertheless, such efforts are still limited in sustaining a high Columbic efficiency because the ductility induced by the limited Cu atoms is not enough to tolerate the volume change that occurs during the charge/discharge reactions, which deteriorates the stability of the interface between the electrode and the electrolyte. Accordingly, it is necessary to find out a remarkable matrix to minimize the morphological changes and to prevent the loss of electronic conductivity during the lithiation/delithiation reactions. Within this concept, Kawakami and Asao (2005) proposed using an amorphous electrode material consisting of SnAX where A is a transition metal and X is at least one of the elements: O, F, N, Mg, Ba, Sr, Ca, La, Ce, Si, Ge, C, P, B, Pb, Bi, Sb, Al, Ga, In, Tl, Zn, Be, Pr, Nd, Sm, Eu, Gd, Tb, Dy, Ho, Er, Tm, Yb, Lu, As, Se, Te, Li, and S. Moreover, Mizutani and Inoue (2005) anticipated this idea by using SnMX systems where M is one of the elements: Ni, Cu, Fe, Co, Mn, Zn, In or Ag; and X is one of the elements: B, C, Al, Si, P, or S. Among these

*Author for correspondence (ozgulkeles@itu.edu.tr)

options, Sn–Co–C-based material, which was commercialized by Sony in 2005, appears to be very attractive (Zhang *et al* 2011). However, since Co is very expensive and toxic, the need for finding alternative anode materials is still under discussion.

In this study, bare Sn and composite Cu–Sn and Cu–Sn–C nanostructured thin film anodes are deposited on Cu discs by glancing angle electron (GLAD) beam evaporation process. GLAD process is chosen particularly because there is no risk of hazardous handling of flammable, explosive or cancerogenous metal nanoparticles; and no need of binder or conductive additives to get a nanosized electrode with nanoporosities. The porosities in the films are expected to significantly improve the performance of the rechargeable batteries since they would provide easy access of the electrolyte to the entire electrode surface. Moreover, it is believed that with the lack of binder, the electrical resistance would be also very low in these films (Kepler *et al* 1999; Belt *et al* 2003; Jung and Lee 2011).

In this study, for the first time in the literature, a nanostructured Cu–Sn–C thin film is produced via the GLAD method, where the evaporation of carbon is achieved in a controlled manner. In this paper, the possible use of the Cu–Sn–C thin film as an anode material is investigated by comparing its electrochemical performance to that of the nanostructured Sn and the nanostructured CuSn thin films. The results clearly demonstrate the positive effects of the porous morphology and the presence of Cu and C in the thin film on the electrochemical performances of the electrodes, in order to fabricate a high-performance Sn-based anode for lithium ion batteries.

2. Experimental

Three Sn containing thin films (pure Sn, Cu–Sn and Cu–Sn–C) were fabricated on Cu discs (15·5 mm diameter, 1·5mm thickness) by using the glancing angle electron beam co-deposition technique. During the deposition process, the base vacuum in the chamber was around 10^{-7} mTorr. Two graphite crucibles were used. Batch compositions in the crucibles for each deposition are given in table 1.

Table 1. Batch compositions in each crucible prior to deposition.

Coatings	Crucible 1	Crucible 2
Sn thin film	Pure Sn pellets	–
Cu–Sn thin film	Mixture of Cu–Sn pellets (2/3 wt%)	–
Cu–Sn–C thin film	Mixture of Cu–Sn pellets (2/3 wt%)	Graphite

In order to produce the nanostructured Sn, Cu–Sn and Cu–Sn–C thin films, first Sn (for bare Sn thin film) or Cu–Sn (for Cu–Sn or Cu–Sn–C thin films) were deposited with an incident flux angle of 0°, because it was believed that the presence of this non-porous (flat) thin film would increase the electrical contact of the nanostructured thin film to the substrate. Then, a subsequent co-deposition of Sn, Cu–Sn, Cu–Sn–C thin films were achieved with an angle of 80° (vs the target's surface normal) on the non-porous layer to form the nanostructured Sn, Cu–Sn and Cu–Sn–C thin films, respectively. The compositions of the film were determined by energy-dispersive X-ray spectroscopy (EDX) analysis and are given in table 2.

The surface morphology of the thin films prior and after the galvanostatic tests were analyzed by utilizing a field-emission scanning electron microscopy (FE-SEM, JEOL JSM 7000F). The samples were washed with dimethyl carbonate (DMC) before the analysis. The phases present in the pristine films were determined by using Philips PW3710 System (with CuKα at 40 kV and 30 mA). The X-ray data were collected in the 2θ range of 20–90° in steps of 0.05°.

Moreover CR2032 coin cells were fabricated to test the electrochemical properties of the electrodes. The cells were assembled in an Argon filled glove-box (MBRAUN, Labmaster). The testing cells were based on the following sequence: (i) a working electrode, (ii) a 1 M $LiPF_6$ in the ethylene carbonate–dimethyl carbonate, EC:DMC 1:1 (Merck Battery Grade) electrolyte solution, (iii) separator (Celgrad 2400) and (iv) a lithium metal foil as a counter electrode.

The cells were tested at room temperature between 5 mV and 2·5 V vs Li/Li^+ with a rate of 50 mA g^{-1}. The cyclic voltammetry (CV) was performed in the potential range of 5 mV–2·5 V vs Li/Li^+ at a scan rate 0·03 mV s^{-1}. The impedance spectra after the first and the third cycles were also recorded in a frequency range of 1000–0·01 Hz with an amplitude of 5 mV.

3. Results and discussion

3.1 *Structural and morphological characterization*

By placing the Cu substrate above a material vapor source at an oblique angle, a nanostructured thin film is fabricated. These nanostructures are oriented towards the vapor source because of the self-shadowing effect and they are

Table 2. Results of EDS analyses on Cu–Sn and Cu–Sn–C thin films.

	Cu		Sn		C	
Coatings	(wt%)	(at%)	(wt%)	(at%)	(wt%)	(at%)
Cu–Sn	53·07	67·87	46·93	32·13	0	
Cu–Sn–C	32·19	29·47	59·24	29·03	8·57	41·50

homogeneously distributed in the thin film because of the limited surface diffusion ability of ad-atoms (Patzig *et al* 2010). Figure 1(a)–(f) reveals the surface and the cross sectional views of the nanostructured Sn, Cu–Sn and Cu–Sn–C thin films.

The pure nanostructured Sn electrode has a remarkable pillar-like structure and the thin film is fairly inhomogeneous in sizes (figure 1a). Its cross sectional view demonstrates clearly that the pillars are not homogeneously deposited on Cu substrate and the thickness is around 150 ± 50 nm (figure 1d). On the other hand, the electrode made of Cu–Sn nanostructured composite thin film has well-aligned composite nanorod arrays where the nanorods' diameters (<100 nm) are very homogeneous (figure 1b). The cross sectional view displays that the resulting film thickness is around 230 ± 20 nm and the interstitial spaces among the nanorods represent homogeneously distributed nanoporosities (figure 1e) in the thin film. For the electrode made of Cu–Sn–C thin film in figure 1(f), no remarkable nanocolumnar structure is detected, but the surface view exhibits the presence of the homogeneously distributed nanosized porosities in the nanostructured thin film.

The comparison between Cu–Sn containing thin films' XRD data with that of Sn displays that an additional amount of Cu enhances the intermetallic formation. Figure 2 displays the presence of Cu-rich Cu_6Sn_5 ($Cu_{6.26}Sn_5$) crystallites instead of Sn nanocrystallites in the CuSn thin film. The high Cu content in the nanocolumnar structured Cu–Sn thin film is also justified by EDS analysis (table 2).

The EDS analysis shows that the thin films have different compositions than the source composition. The difference between the source and the thin film composition can be explained as being an outcome of the evaporation point differences of the metals at constant pressure and the nature of the GLAD method. Because in the GLAD method, the deposition rate not only has a vertical component (with respect

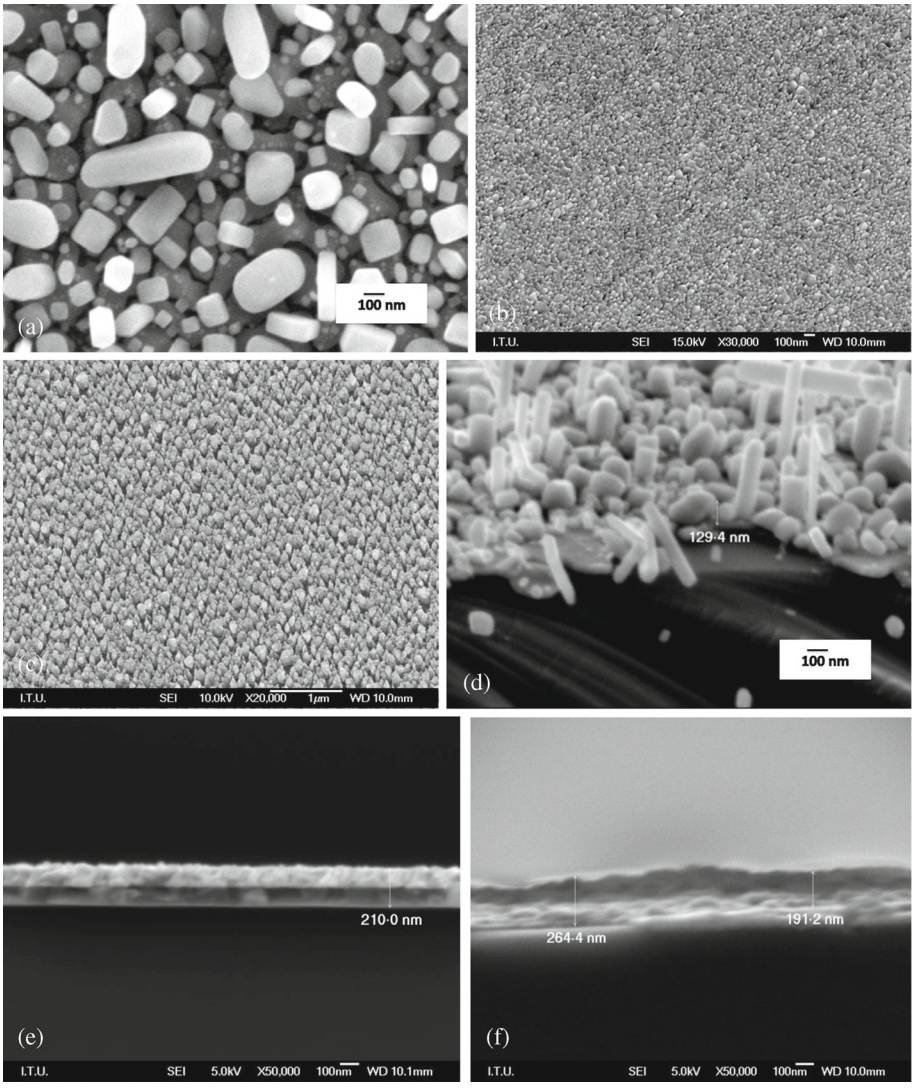

Figure 1. SEM surface views of nanostructured (**a**) bare Sn, (**b**) Cu–Sn, (**c**) Cu–Sn–C thin films; SEM cross sectional views of nanostructured (**d**) bare Sn, (**e**) CuSn and (**f**) Cu–Sn–C thin films.

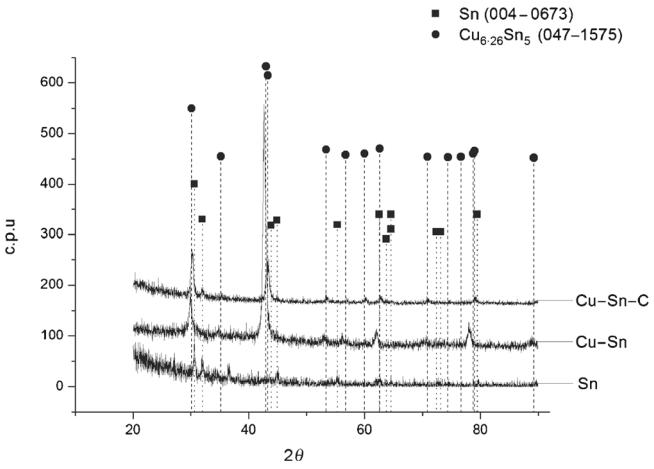

Figure 2. XRD analyses results of nanostructured bare Sn, Cu–Sn and Cu–Sn–C thin films.

to the substrate surface), but also has a lateral component, which in turn forms thin films with different compositions and thicknesses (Derrien *et al* 2007). Moreover, figure 2 demonstrates the small peak shift in the Cu–Sn film, which may be explained by the internal stress of the thin film due to the existence of the excessive amount of Cu atoms in the Cu_6Sn_5 crystal. However, the XRD data of Cu–Sn–C containing thin film shows no peak shift because of the presence of C in the thin film, which results in a reduction of the grain size of forming the nanostructured thin film electrode. The fact that there is a broadening in the Sn peak at 30·645° and a decrease in its intensity also supports the grain refiner effect of the carbon atom. Moreover, the absence of the characteristic peak at 89·7° for $Cu_{6.26}Sn_5$ justifies that an excessive Cu is not present in the crystal of Cu_6Sn_5 for Cu–Sn–C thin film. When the XRD data of the Cu–Sn–C is observed in detail, no peak related to the presence of carbon is noted, which could be related to the amorphous phase of carbon as revealed by the presence of a bump at low diffraction angles.

3.2 *Electrochemical characterization*

The cyclic voltammograms (CV) of the pristines Sn, Cu–Sn and Cu–Sn–C thin films are shown in figure 3(a)–(c). The reduction peaks related to the formation of Li–Sn materials, and the anodic peaks corresponding to Li de-alloying reactions are detected for all thin films. For the nanostructured Sn thin film, one irreversible and two reversible reduction peaks are observed around 0·7, 0·5 and 0·3V vs Li/Li^+, which are related to the electrolyte reduction (to form SEI), and Li–Sn alloys (with Li-deficient and Li-rich phases) formation, respectively (Jung and Lee 2011). The anodic peaks detected in figure 1(a) show that the first discharge reaction is partially reversible, resulting in the recovery of Sn partially from the lithiated products. For the Cu–Sn thin film, the reduction peaks around 0·3 and 0·1 V indicate the formation of Li–Sn (Li-rich) alloys formation. The anodic peaks noted around 0·5 and 0·7 V demonstrate that the SEI layer might

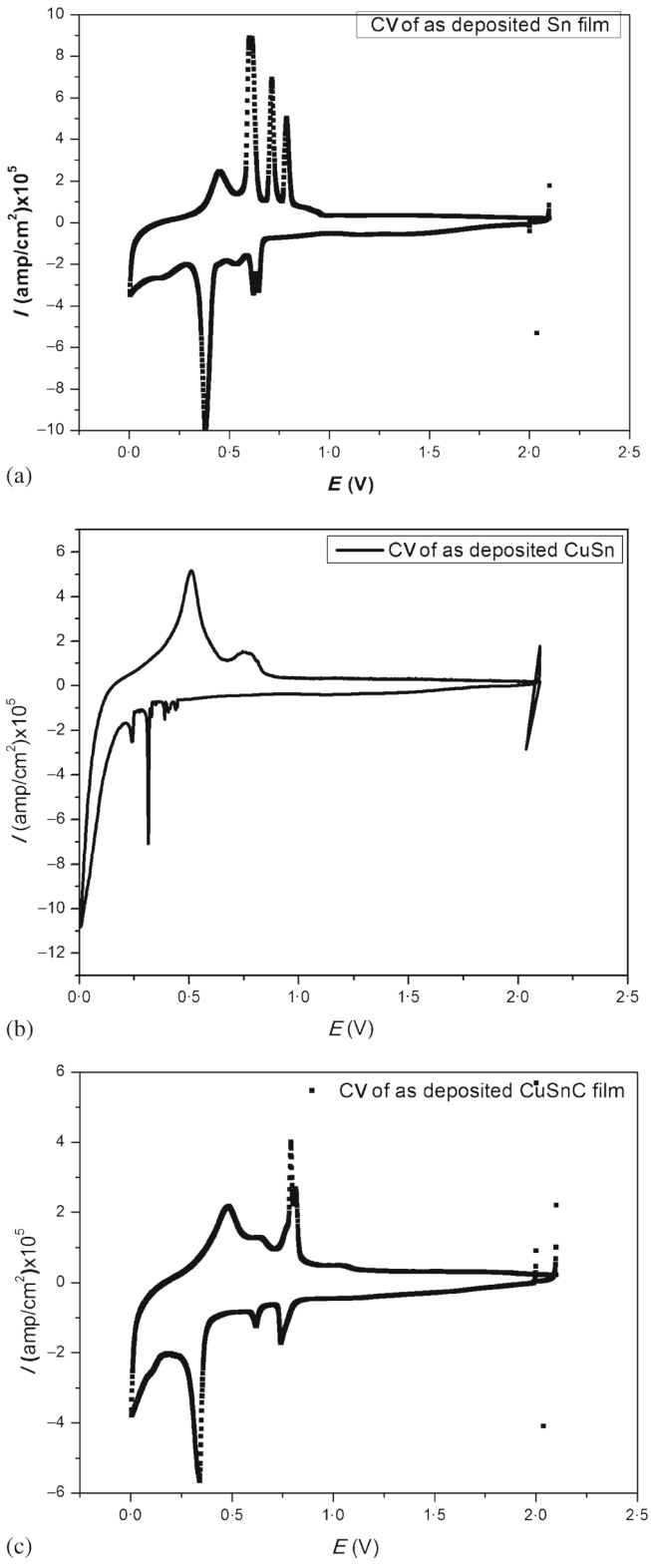

Figure 3. CV analyses of the as deposited nanostructured (**a**) bare Sn, (**b**) Cu–Sn and (**c**) Cu–Sn–C thin films.

form during the reduction process, since the first discharge reaction is not fully reversible. The first cycle CV data of the nanostructured Cu–Sn–C thin film justifies the formation of the SEI on the electrode surface (figure 3c) with a reduction

peak observed at 0·8 V. The other cathodic (∼0·6, ∼0·3 and ∼0·0 V) and the anodic peaks (∼0·5, ∼0·6 V) show the lithiation/delithiation of the Cu–Sn–C electrode according to (1) and (2) (Shin and Liu 2005).

When the CV data of all the nanostructured thin films are compared, it is possible to discuss the effect of Cu and/or C on the thin film's electrochemical performance: Cu has no effect on the peak positions, which justifies that it is inactive when reacting with Li; and C enhances the activity of Li^+ since the oxidation and reduction peak intensities are much higher than those of the nanostructured Sn and CuSn thin films. Moreover, it seems highly possible to have the SEI formation on the three electrodes' surfaces after the first discharge reaction; because the first lithiation/delithiation reactions have a very high irreversibility.

The complex impedance spectroscopic analysis of the three nanostructured Sn-based thin films after the first and third discharge reactions display the presence of a semicircle at high frequency region, which represents the lithium ion interfacial transfer resistance, and a line having a slope of 45° angle at low frequency region shows the existence of solid-state diffusion of Li^+ into the bulk material. Figure 4(a) demonstrates that the nanostructured Sn thin film has two semicircles on the EIS data after the first cycle, which proves that the nanostructured film has multiple interfaces with the electrolyte. After the first cycle, the semicircles gather together to form one circle at the high frequency region and the charge-transfer resistance noted after the third cycle decreases compared to that of the first cycle. This change in impedance could be explained considering the pulverization of the thin film due to high volume changes which in turn distort the film morphology (the pillar morphology is lost, leading to small size particles containing thin film) and the interfaces between the thin film and the electrolyte are settled together eventually. This increase in nanostructured Sn thin film's surface area during cycling affects the detected amount of the current in the impedance. This rise in the current recovered from the electrode could explain the decrease in the impedance of the cells after the 3rd cycle. On the other hand, the impedance data of the nanostructured Cu-Sn thin film reveals that an additional semi-circle is formed on the EIS data of the 3rd cycle, where the real impedance value between the current collector and the thin film also decreases. This behavior proves that a partial delamination of the Cu–Sn nanorods containing thin film occurs after three cycles, due to the volumetric change. Besides, figure 5(a) shows that even the volume of the Cu–Sn thin film increases during lithiation, the film does not delaminate entirely thanks to the improved adhesion (due to the presence of Cu) and the homogeneously distributed porosities in the composite thin film. When the EIS data (both the as-deposited and after the 3rd cycle) of the nanostructured Cu–Sn–C thin film are observed in detail, a decrease in the internal resistance is detected, whereas the real impedance at the interface remains slightly constant. Previous work shows experimentally that C is generally present in the SEI film that forms on the electrode after the first discharge reaction and remains mostly on the surface during the cycling test (Wang *et al* 2006). Thus, the expected presence of C in the SEI covering the entire electrode surface could work as binder in the thin film,

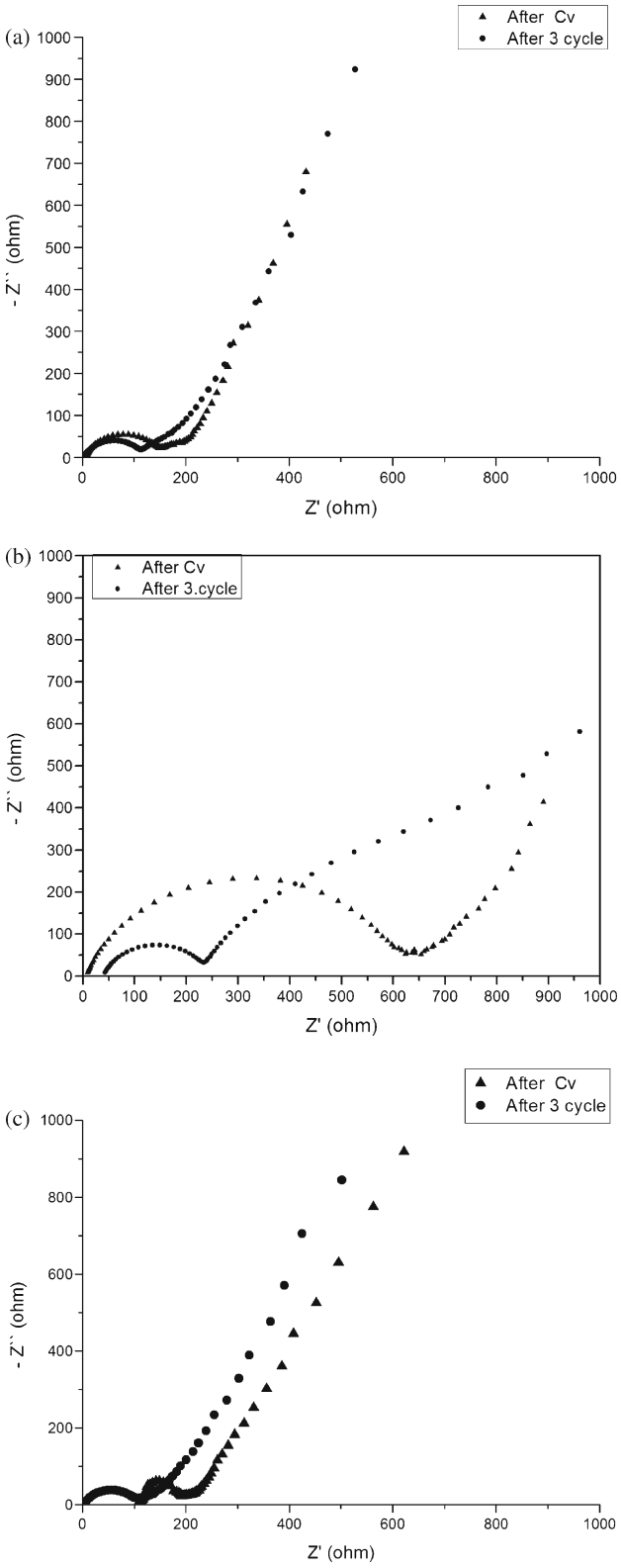

Figure 4. EIS spectra of the as deposited nanostructured (**a**) bare Sn, (**b**) Cu–Sn and (**c**) Cu–Sn–C thin films.

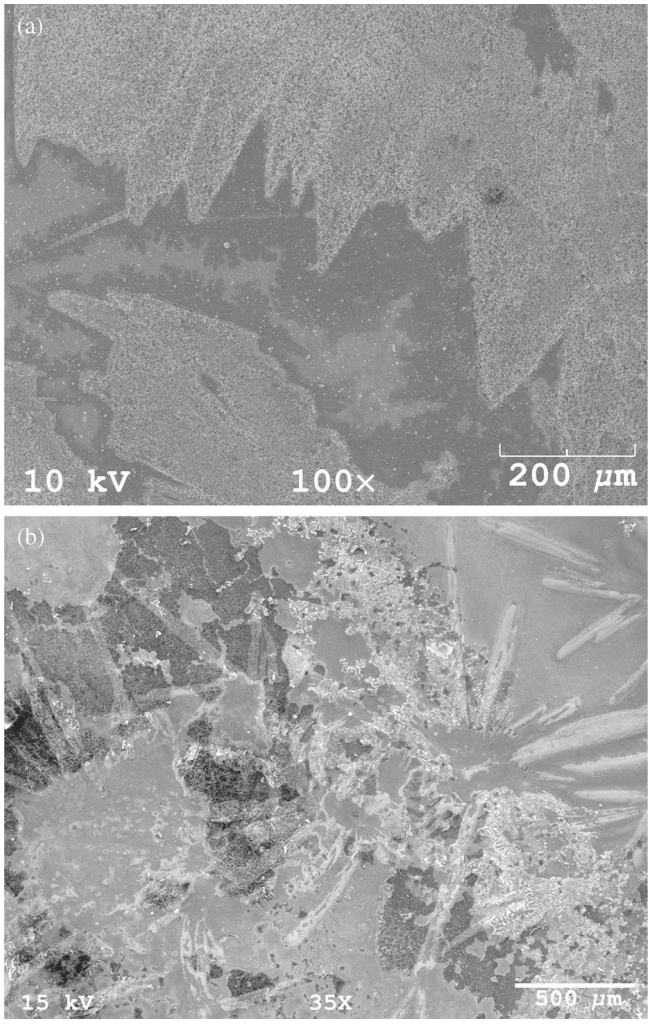

Figure 5. SEM images of (**a**) the Cu–Sn and (**b**) Cu–Sn–C thin films after 80th cycles.

which decreases the internal resistance of the film after the 3rd cycle. The SEM surface view of the Cu–Sn–C thin film after 80 cycles justifies the partial delamination in the thin film and the pulverization occurs on the remaining part of the electrode (see figure 5b).

In figure 6(a)–(c), the galvanic charge–discharge test results of the nanostructured Sn, Cu–Sn and Cu–Sn–C thin film anodes are given. The nanostructured Sn film demonstrates the first discharge capacity around 980 mAh g^{-1}, which is almost equal to the theoretical capacity of Sn (figure 6a). The capacity diminishes gradually in the following 20 cycles. Once the capacity is 450 mAh g^{-1}, a steady state regime is started and reined up to 50th cycles (figure 6a). This gradual decline in the capacity can be explained considering the pulverization of the inhomogenously distributed pillar like Sn particles during lithiation/delithiation reactions. The Columbic efficiency of the anode is around 90% after the first cycle, which shows that the interaction of the thin film with the electrolyte is not stable under the testing conditions and a continuous loss of Li^+ present in the cell during cycling.

The capacity values in the graphs of Cu–Sn and Cu–Sn–C thin films are calculated based on the active material present in the thin films. Considering the theoretical capacity of Sn and its composition (table 2); the theoretical capacity of the Cu–Sn thin film is found as 465 mAh g^{-1} ($991 \times 0{\cdot}4693 = 465$). This value is lower than the initial discharge capacity of the sample (800 mAh g^{-1}). Chiu *et al* explain this fact by the formation of the SEI, which is formed once the active elements react with Li^+ from the electrolyte (Thackeray *et al* 2005). When figure 6(b) is analyzed in detail it is seen that the Cu–Sn composite thin film having homogeneously distributed nanorods array demonstrates a decrease in the capacity that occurs at the very beginning of the cycling test (in the first 3 cycles, Coulombic efficiency around 60%) and once the capacity goes down to 300 mAh g^{-1}, it becomes almost stable upto 80th cycle (Coulombic efficiency around 99%). This decrease in capacity might be attributed to the reduction of the electrolyte and the subsequent SEI formation on the thin film surface as mentioned previously. Once a stable SEI layer is formed on the anode surface, the decay in the capacity disappears and a steady-state regime of the charge–discharge capacity is reached (see figures 6b), eventually.

When the electrochemical performance of the nanostructured Cu–Sn–C thin film is observed (figure 6c), the first cycle in Columbic efficiency is around 70%, which then increases to 99·5% after 20 cycles. The theoretical initial discharge capacity of Cu–Sn–C thin film can be calculated considering the additional capacity coming from the presence of C (theoretical capacity: 372 mAh g^{-1}), resulting in 618·95 mAh g^{-1} ($(991 \times 0{\cdot}5924) + (372 \times 0{\cdot}0857) = 618{\cdot}95$ mAh g^{-1}) as the first discharge capacity in total. This theoretical value is lower than the value shown in figure 5(c) (900 mAh g^{-1}), which could be also explained, considering the SEI layer formation in the thin film surface (Jung and Lee 2011). The improved cycle retention and the high Columbic efficiency (>99%) detected after the first cycle can be related to the existence of additional C in the thin film, leading to a higher electrochemical performance of 450 mAh g^{-1} upto 80 cycles.

Figure 6(d) displays the comparison of cycle number dependence of the insertion and extraction capacities among all the thin films. All the three thin films have a low first cycle Columbic efficiency (<80%). SEI layer formation might be a possible explanation for it. However, other possible series of irreversible processes can also lead to the first cycle irreversible capacity change: (i) the inability of extruded Cu to re-incorporate into Sn structure, (ii) the inconsistency in the 'rearrangement' of the electrode structure depending on the carbon presence and (iii) a possible contact loss between the thin film and the current collector due to the volume change (Li *et al* 2002; Wang *et al* 2007). The comparison also reveals that even all the three samples are fabricated via GLAD method and have a large surface area to reduce the local current density and decrease polarization, they perform different performances due to their different compositions and indeed their structures and morphologies. As mentioned previously, the porosity in the thin films changes

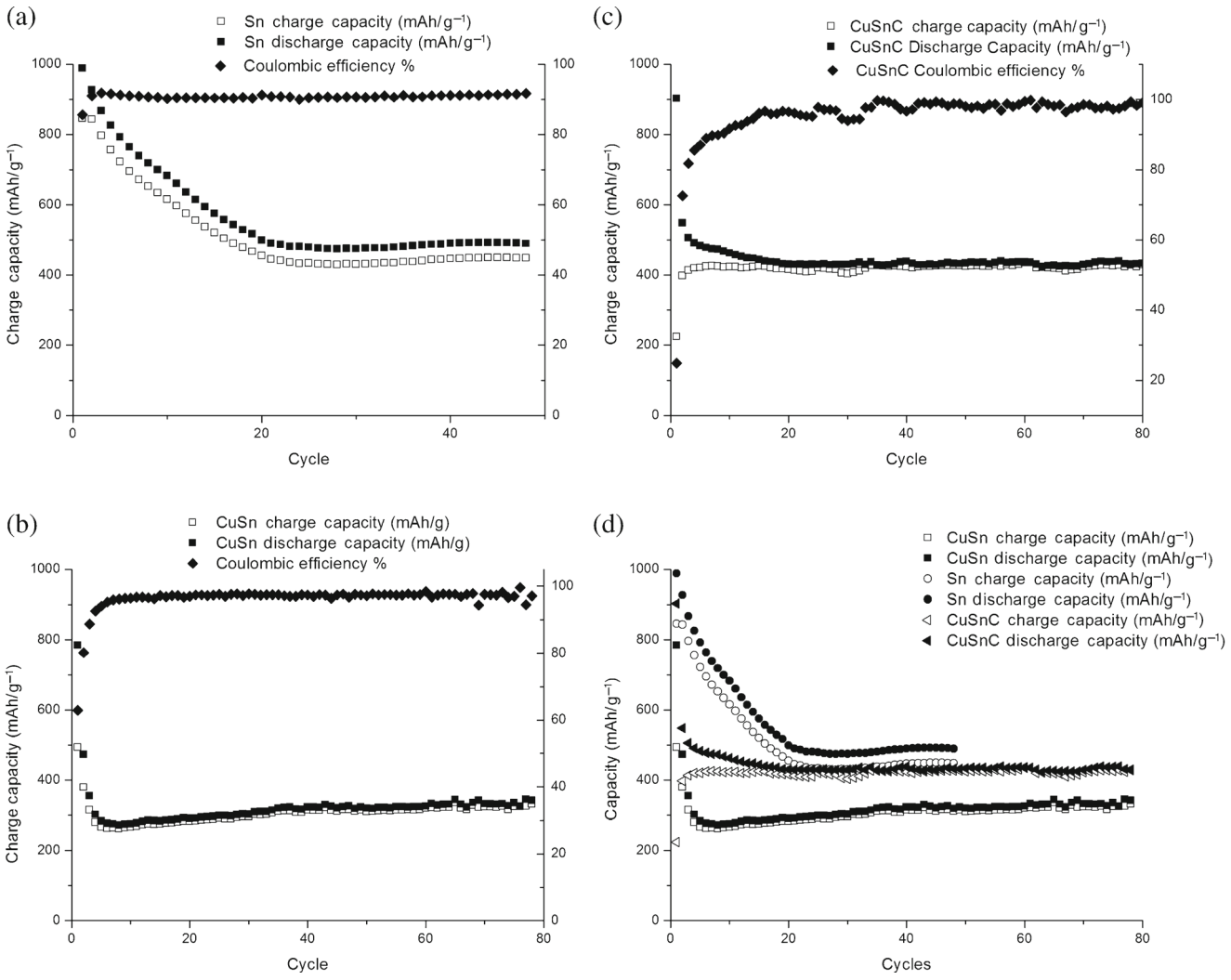

Figure 6. Discharge–charge capacities of the as deposited nanostructured (**a**) bare Sn, (**b**) Cu–Sn, (**c**) Cu–Sn–C thin films upon cycling and (**d**) comparison of electrochemical performances of Sn, Cu–Sn and Cu–Sn–C thin film anodes.

depending on their morphology, and the structure depends on the nucleation and growth mechanisms of the evaporated particles. Thus, the Cu addition which enhances the composite nanorod formation in the thin film, facilitates Li^+ movement within the electrode and shortens the Li^+ diffusion distances. Added to this, the excessive amount of Cu having a buffering effect improves the tolerance of the thin films against the drastic volume change because of its ductile properties and increases the electrical conductivity of the thin films due to its conductive behavior to promote the charge transferring reactions of the electrode during cycling test (Shin and Liu 2005; Thackeray *et al* 2005). Figure 6(d) also reveals that the presence of C augments the Coulombic efficiency of the sample once a stable oxide layer forms on the electrode. This could be explained referring to SEI composition analyses, where the presence of C in the thin films improves the electrical and mechanical properties of SEI layer, which improves the electrochemical performance of the anode as well (Wang *et al* 2006).

4. Conclusions

In this paper, the oblique angle deposition process is used to produce nanostructured Sn, Cu–Sn and Cu–Sn–C thin films.

The results of this work can be summarized as follows:

(I) GLAD method is a useful method to produce nanostructured Sn-based thin films. The production process may open a new area of research for the development of metal storage electrodes since there is no risk of hazardous handling of flammable, explosive or cancerogenous metal nanoparticles; and no need and limitation of (traditional) binder or conductive additives. We believe that this composite thin film with nanoporosities will have use as potential anode material in lithium battery storage.

(II) To our knowledge, up to now, there is no published work in which a carbon contained nanostructured Cu–Sn thin film is produced by using an oblique angle deposition method.

(III) Pure Sn nanorods have a higher initial anodic capacity of 980 mAh g^{-1}, but the capacity diminishes after 20 cycles due to the morphological changes. When the cycling is continued upto 50th cycles, then it failed.
(IV) A remarkable nanostructured Cu–Sn–C thin film made of small particles with homogeneously distributed porosities is formed by using the GLAD method. Initial discharge capacity is found to be around 900 mAh g^{-1}, then a gradual decrease is noticed upto 20th cycles, then after 20 cycles the capacity becomes fairly constant around 450 mAh g^{-1} upto 80th cycles.

Acknowledgements

This work is a part of the research project 110M148 approved by The Scientific and Technological Research Council of Turkey (TUBİTAK). The research grant is gratefully acknowledged.

References

Belt J R, Ho C D, Motloch C G, Miller T J and Duong T Q 2003 *J. Power Sources* **123** 241

Besenhard J O, Komenda P, Paxinos A, Wudy E and Josowicz M 1986 *Solid State Ionics* **18–19** 823

Besenhard J O, Yang J and Winter M 1997 *J. Power Sources* **68** 87

Chen C K, Zhang X F and Cui Y 2008 *Nano Lett.* **8** 307

Derrien G, Hassoun J, Panero S and Scrosati B 2007 *Adv. Mater.* **19** 2336

Jung H R and Lee W J 2011 *J. Electrochem. Soc.* **158(A)** 644

Kamali A R and Fray D J 2011 *Recent Adv. Mater. Sci.* **27** 14

Kawakami S and Asao M 2005 *US Patent Application* 6 949 312

Kepler K D, Vaughey J T and Thackeray M M 1999 *Electrochem. Solid-State Lett.* **2** 307

Lee K 2007 *Synthesis of Si nanowires for an anode material of Li batteries, Ph.D Thesis* (Korea: Pohang University of Science and Technology) p 13

Li H, Shi L H, Wang Q, Chen L Q and Huang X J 2002 *Solid State Ionics* **148** 247

Lindsay M J, Wang G X and Li H K 2003 *J. Power Sources* **119** 84

Mizutani S and Inoue H 2005 *US Patent Application* 0208378

Patzig C, Miessler A, Karabacak T and Rauschenbach B 2010 *Phys. Status Solidi B* **247** 1310

Shin H-C and Liu M 2005 *Adv. Finct. Mater.* **15** 582

Thackeray M M, Vaughey J T and Fransson L M L 2005 *JOM* **54** 20

Wang J, Ng S-H, Wexter D, Konstantinov K, Guo Z-P and Liu H-K 2006 *Angew. Chem. Int. Ed.* **45** 6896

Wang F, Zhao M and Song X 2007 *J. Alloys Compd.* **439** 249

Wachtler M, Besenhard J O and Winter M 2001 *J. Power Sources* **94** 189

Zhang R, Upreti S and Whittingham M S 2011 *J. Electrochem. Soc.* **158** A1498